ELSEVIER

Journal of Nuclear Materials 304 (2002) 8–14

journal of nuclear materials

www.elsevier.com/locate/jnucmat

Influence of dilute silicon addition on the oxidation resistance and tensile properties of modified Zircaloy-4

Hyun Seon Hong *, Seon Jin Kim, Kyung Sub Lee

Department of Materials Science and Engineering, Hanyang University, Seoul 133-791, South Korea

Received 11 February 2002; accepted 10 May 2002

Abstract

Si-added modified Zircaloy-4 (Zry-4) and Zr–Si binary alloys were developed to evaluate the effect of silicon addition on zirconium based alloys for high burn-up application. The silicon content varied from 0 to 0.1 wt% for both the alloys. The relationships between alloy chemistry, microstructure, mechanical property and oxidation behavior were investigated. The ultimate tensile strength of the modified Zry-4 generally increased with the increase in silicon content. The optimum silicon content for improved oxidation resistance turned out to be 0.01 wt% from the weight gain measurement. The weight gain decreased with decreasing Si content from 0.1 to 0.01 wt% although the Si free specimen showed higher weight gain than the 0.01 wt% Si specimen. The details of microstuctural change with silicon addition and its influence on tensile properties and oxidation resistance are discussed; the effects of silicon on the oxide crystal structure, second phase precipitates and microstructure of the metal matrix are studied.

1. Introduction

Zircaloy-4 (Zry-4) has been widely used as a cladding material in pressurized water reactors. However, the trend to extended cycle lengths with high coolant lithium level has led to an increased demand on the oxidation resistance and the mechanical property of the cladding material. It was recently found that the oxidation resistance of Zry-4 was improved by the reduction of the tin content; however, the decrease in tin content degraded the mechanical properties such as ultimate tensile strength and yield strength. Based on these results zirconium alloys containing a potential alloying element such as Nb, Mo and V have been designed for advanced cladding materials [1–5]. It was reported that the oxidation resistance of the zirconium-base alloys improved by a small addition of Nb (about 0.05–0.2 wt%) compared to that of Zry-4 [6–8] and the small addition of Mo and V resulted in a further improvement of the mechanical properties without a considerable degradation of oxidation resistance. In addition, correlations between alloying elements, processing, microstructure, and oxidation behavior were studied in these binary alloys.

The authors have participated in that research for some years and have already published previous results on the oxidation and the mechanical properties of oxygen- and copper-added modified Zry-4 alloys [9–14]. The studies were related to a specific point of view, namely to the increase of the strength of Zry-4 and the enhancement in the oxidation resistance by alloying with oxygen and copper as a potential substitute of tin. The addition of small amounts of oxygen turned out to improve the mechanical properties but degraded the oxidation resistance. However, the addition of copper was reported to improve the mechanical properties without sacrificing the oxidation resistance. The addition of around 0.1–0.2 wt% Cu rather exhibited the slight improvement of the oxidation resistance.

The present study is part of the authors' continuing research in finding the optimum content of alloying

* Corresponding author. Tel./fax: +82-2 2281 4914.
E-mail address: hshong@ihanyang.ac.kr (H.S. Hong).

0022-3115/02/$ - see front matter
PII: S0022-3115(02)00875-9

elements for improving the mechanical and oxidation properties of cladding materials. In this study, the effects of silicon addition on the tensile and the oxidation properties of the modified Zry-4 are investigated. To assess the influence of silicon addition on the oxidation behavior, autoclave oxidation tests in pure water at 360 °C were conducted up to 100 days and weight gain changes were observed as a measure of the oxidation resistance. In addition, tensile tests at room temperature were performed and the microstructural parameters such as oxide structure, precipitate distribution, and grain structure were characterized with increasing silicon content.

2. Experimental procedures

2.1. Specimen preparation

Three types of zirconium alloys containing silicon were prepared. In the first class, specimens have the standard tin content of Zry-4 (1.5 wt% Sn). The Fe/Cr ratio of the specimens was maintained at either 2 or 0.5. The silicon content varied from zero up to 0.1 wt%. In the second class, the tin content was reduced to 1.0 wt% and the Fe/Cr ratio was maintained at 2. In addition, the silicon content increased from zero to 0.1 wt%. In the third class, Zr–Si binary specimens were prepared by changing the silicon content from zero to 0.1 wt%. The chemical compositions of the present specimens are listed in Table 1.

The specimens were prepared according to the following procedures. Pure reactor grade sheet-type Zr and alloying elements were arc melted into 100 g button type ingots. The homogenized ingots were beta forged at 1010 °C and quenched into water. After the beta quenching, the ingots were hot-rolled at 700 °C and annealed at 650 °C under an argon atmosphere. The plates were then cold-rolled and annealed at 700 °C for 1h for recrystallization. The oxide scale formed on the plates during these thermomechanical treatments was removed by mechanical polishing and pickling in a mixed solution of 10% HF, 45% HNO_3 and 45% H_2O before the test specimens were machined to their final shapes.

Table 1
Chemical composition (in wt%) of the Si-added Zr alloys

Specimen number	Alloying elements				
	Sn	Fe	Cr	Si	Zr
1	1.5	0.2	0.1	0.0	Balance
2	1.5	0.2	0.1	0.01	Balance
3	1.5	0.2	0.1	0.1	Balance
4	1.5	0.1	0.2	0.0	Balance
5	1.5	0.1	0.2	0.01	Balance
6	1.5	0.1	0.2	0.1	Balance
7	1.0	0.2	0.1	0.01	Balance
8	1.0	0.2	0.1	0.05	Balance
9	1.0	0.2	0.1	0.1	Balance
10	0.0	0.0	0.0	0.01	Balance
11	0.0	0.0	0.0	0.05	Balance
12	0.0	0.0	0.0	0.1	Balance
13	Conventional Zry-4				

2.2. Tensile test

Tensile tests were performed at room temperature at a strain rate of 5.2×10^{-4} s^{-1} by using a SATEC tensile testing machine with the maximum load capacity of 10 000 kg. The tensile test specimens were made along the rolling direction with a gauge length of 25 mm, a width of 6 mm and a thickness of 1 mm. The specimens were mechanically and chemically polished in a solution of 10% HF, 45% HNO_3 and 45% H_2O in order to remove any surface defects. A total of three runs per each specimen were carried out and both of the ultimate tensile stress and the yield stress were measured. The standard deviation of the results was ± 5 MPa.

2.3. Microstructural analysis of precipitates

Scanning electron microscopy (SEM) and scanning transmission electron microscopy (STEM) were performed to characterize the precipitates in the metal phase before the oxidation test. The crystal structure was determined by selected area electron diffraction pattern, and the quantitative analysis of precipitates was performed using STEM with energy dispersion spectroscopy (EDS). It is a useful instrument for analyzing chemical compositions of intermetallic precipitates smaller than 10 nm because the small size of the beam probe ($\approx$20 nm) permits excellent spatial resolution by centering the beam within the particle of interest. STEM samples were mechanically polished to 50 μm and jet-polished in a solution of 90% ethanol and 10% perchloric acid at −40 °C and 13 V. SEM samples were etched in a solution of 5% HF, 45% HNO_3 and 50% H_2O.

2.4. Oxidation test

The specimens for the oxidation test were prepared by the procedures described in the previous study [9,12,14]. The oxidation tests were conducted in autoclaves filled with pure water at 360 °C under a pressure of 180 bar. Oxidation test specimens with the dimension of 10 mm × 25 mm × 1 mm were prepared from the recrystallized sheet specimens. The specimens were mechanically and chemically polished before testing. The test followed the ASTM G2 method [15]. The oxidation

behavior was evaluated by the weight gain (ΔW) as a function of exposure time.

2.5. Oxide analysis

In order to identify the crystal structure of the growing oxide surface Raman spectroscopy was used. The methods of characterization of the ZrO_2 structure by a Raman spectrometer have been reported elsewhere [16–18]. A Raman spectrometer with 200 mW argon-ion laser source at a wavelength of 488 nm was used. The spectral range employed was from 100 to 500 cm^{-1}.

3. Results and discussion

3.1. Tensile tests

Changes of UTS as a function of the silicon content for the modified Zry-4 are presented in Fig. 1. The UTS of the specimens generally increased with the silicon content. In case of specimens containing 1.5 wt% Sn, as the silicon content increased from 0 to 0.1 wt%, the UTS increased from 486 to 503 MPa. The specimen with 1.0 wt% Sn showed a similar result to that of the specimen with 1.5 wt% Sn (from 435 to 465 MPa). The change in UTS with the present silicon contents is about 4–7%, which is found to be slightly smaller than that with the tin contents (8–12% change in UTS). Changes of YS showed a similar trend to UTS. The results of the tensile tests are summarized in Table 2.

In Fig. 1, the strengthening effect of silicon on UTS is compared to that of copper and oxygen [9,13]. As can be seen in the slope of the lines, the effect of copper and oxygen on the increase of the UTS is higher than that of silicon. In the previous study it was found that the increase in strength due to the addition of 0.1 wt% oxygen or copper is sufficient to compensate the decrease in strength due to the reduction of the tin content from 1.0 to 0 wt%. However, it seems that 0.1 wt% silicon in the present study cannot make up the reduction of the tin content from 1.5 to 1.0 wt%.

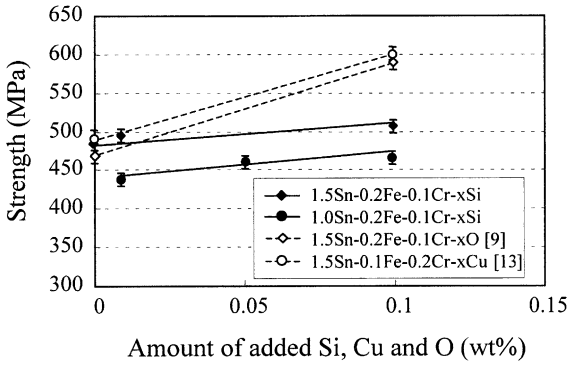

Fig. 1. UTS as a function of silicon, copper, and oxygen at room temperature.

Table 2
Mechanical properties of the modified Zry-4 alloys

Specimen number	Tensile properties		
	UTS (MPa)	YS (MPa)	Elongation (%)
1	486	362	23
2	491	370	22
3	503	374	21
4	488	364	23
5	496	372	22
6	518	396	19
7	435	332	28
8	460	335	25
9	466	340	22

Although the phase diagram of the zirconium-silicon system has been extensively studied, the solubility of silicon in alpha zirconium at room temperature has not yet been clarified [19–22]. However, it can be estimated by using the terminal solubility equation, $C = C_0 \times \exp(-\Delta H/RT)$. The solubilities of silicon at 863 °C and at 1570 °C are reported to be 0.09 and 0.18 wt%, respectively. From these data the ΔH and the C_0 values can be determined, and the solubility of silicon at room temperature is calculated to be about 5.1×10^{-4} wt%. Therefore, the lowest silicon content (0.01 wt%) used in this study is considered to be far above the solubility limit of silicon at room temperature. Accordingly, it is considered that silicon precipitates induced the increase in strength. The strengthening effect of the precipitates is discussed more in Section 3.3.

3.2. Weight gain

Fig. 2 shows the weight gain change with the silicon content for the Zr–Si binary alloy and the modified Zry-4 alloys. In case of the Zr–Si binary alloy, as seen in the graph, the weight gain was reduced as the silicon content decreased from 0.1 to 0.01 wt% within 50 days exposure. However, the weight gain of the silicon free specimen was higher than that of the 0.01 wt% Si specimen; the specimen containing 0.01 wt% Si showed the lowest weight gain. Fig. 2 shows also the weight gain vs. silicon content in the modified Zry-4 alloy with the Fe/Cr ratio of 0.5 after 100 days exposure. When the silicon content lowered from 0.1 to 0.01 wt%, the weight gain decreased. When the silicon content decreased further to zero then the weight gain slightly increased. In case of the modified Zry-4 alloy with the Fe/Cr ratio of 2 after 100 days exposure, as the silicon content increased from 0 to 0.01 wt%, the weight gain decreased. However, further addition of 0.1 wt% silicon increased the weight gain. This

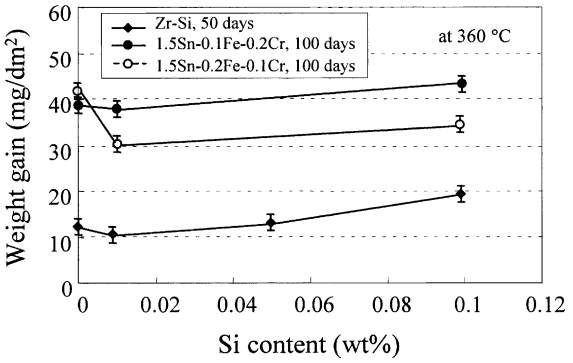

Fig. 2. The weight gain vs. silicon content curve for Zr–Si binary alloys, Zr–1.5Sn–0.1Fe–0.2Cr–*x*Si alloys and Zr–1.5Sn–0.2Fe–0.1Cr–*x*Si alloys.

result is consistent with the trends obtained from the Zr–Si binary alloy and the modified alloy with the Fe/Cr ratio of 0.5.

It is to be noted that the weight gain of the modified Zry-4 alloys is equivalent or slightly lower than that of conventional Zry-4; after 100 days the weight gain of Zry-4 measured in the same autoclave testing condition was about 40 mg/dm^2. Conclusively, it is considered that the dilute silicon addition around 0.01 wt% could improve the oxidation resistance of silicon-added zirconium alloys. The tendency for the optimum content is also observed in the Zr–Nb and Zr–Cu systems [7,14]. A small addition of Nb (around 0.05–0.2 wt%) or Cu (around 0.1–0.2 wt%) improved the oxidation resistance of zirconium-base alloys compared with that of Zry-4. The weight gains of Zr–0.2 wt% Cu alloys were lower by 30% than that of Zry-4.

The oxidation rate exponents (n) obtained from the log–log plots of $W^n = kt$ where W, k, t are weight gain, rate constant, and time, respectively, were in the range of 2.6–3.9 indicating that the alloys followed the cubic rate law. The oxidation kinetics of silicon-containing zirconium alloys studied in this work were, therefore, thought to be similar to that of conventional Zry-4. The weight gains measured are based on short-term experiments. In many cases, the long-term characteristic of weight gain follows the tendency of the short-term characteristic. However, long-term behavior like weight gain in the post-transition region can be different from short-term characteristics. Thus it is necessary to verify the oxidation characteristics of the modified Zry-4 alloys in the long-term experiment.

3.3. Second phase precipitates

The types of the present precipitates were identified using STEM and EDS. For Zr–Si binary alloys, only one type of precipitates, the C16-type tetragonal Zr_2Si, was observed. However, for modified Zry-4 alloys, two types of precipitates were found, that is, (1) C14-type hexagonal $Zr(Fe,Cr)_2$ in both the Si-added and the Si-free alloys or $Zr(Fe,Cr,Si)_2$ in the Si-added alloys, (2) C16-type tetragonal Zr_2Si in 0.1 wt% Si-added alloys. The Zr_2Si precipitate was not observed in the 0.01 wt% Si-added specimen but observed in 0.1 wt% Si-added specimen. Thus it seems that $Zr(Fe,Cr)_2$ is primarily formed in the modified Zry-4 alloys, and then the $Zr(Fe,Cr,Si)_2$ precipitate is formed by replacing Fe or Cr in $Zr(Fe,Cr)_2$ with Si. At the last stage residual Si forms Zr_2Si precipitates in the modified Zry-4 with 0.1 wt% Si addition.

The intermetallic precipitate of $Zr(Fe,Cr)_2$ is known to have either the C14 hexagonal or the C15 cubic structure depending on its relative composition of Fe and Cr [23–29]. According to Malakhova [30], only hexagonal exists when the Fe/Cr ratio ranges from 0.58 to 4.2 whereas both hexagonal and cubic exist when the ratio is in the range of 4.2–10. Similarly, Charquet et al. [31] reported that the precipitates observed correspond to hexagonal for the ratio less than about 4. The present investigations are in agreement with these results; only the C14 hexagonal $Zr(Fe,Cr)_2$ precipitate was observed in all modified Zry-4 alloys (in the ratio range of 0.5–2). The relative portion of Fe and Cr in the precipitate was fairly close to its nominal value in the alloy.

From the Zr–Si binary phase diagram [19–22], Zr-rich intermetallic phases are found to be a stable Zr_2Si precipitate, a metastable Zr_3Si precipitate and a metastable Zr_5Si_3 precipitate. The heat of formation of Zr_2Si precipitate was reported to be around -69.7 kJ/g atom, while that of Zr_3Si and Zr_5Si_3 to be -52.3 and -76.9 kJ/g atom, respectively [32–35]. Although Zr_2Si precipitates have a little difference in the heat of formation from Zr_3Si and Zr_5Si_3 precipitates, in this study any metastable precipitates were not observed but only stable Zr_2Si precipitate was observed in the final structure.

The average size and the area fraction of the precipitates in this study generally increased with increasing Si content. In Zr–Si binary alloys, the size increased from 0.12 to 0.38 μm and the area fraction increased from 1.33% to 4.02% with increasing the Si content from 0.01 to 0.1 wt%. In case of specimens with Fe/Cr ratio of 2, the size increased from 0.12 to 0.14 μm and the area fraction 1.95% to 2.16% as the Si content increased from 0 to 0.1 wt%. The specimens with the Fe/Cr ratio of 0.5 showed the similar result to those with the ratio of 2 as shown in Table 3.

The size of precipitates in the Si-free specimen was a little larger than that in the Si-added specimen. It is thought that the Si addition resulted in a refinement of precipitate in the modified Zry-4 because Si is not very soluble in β- or α-Zr and plays a role in nucleating the phases during the heat treatment. The role of Si in the precipitate of the present specimen is considered to form a Zr–Si binary precipitate or to replace Fe or Cr in $Zr(Fe,Cr)_2$ precipitate, and thus to increase the average

Table 3
Size and area fraction of precipitates in the modified Zry-4 alloys

Specimen number	Particle size (μm)			Area fraction (%)
	Average	Minimum	Maximum	
1	0.12	0.04	0.27	1.95
2	0.11	0.04	0.34	1.86
3	0.14	0.03	0.52	2.16
4	0.09	0.03	0.25	1.23
5	0.09	0.04	0.25	1.15
6	0.13	0.05	0.49	2.25
7	0.11	0.04	0.27	1.48
8	0.13	0.04	0.51	2.09
9	0.14	0.03	0.52	2.34
10	0.12	0.05	0.22	1.33
11	0.16	0.06	0.41	1.79
12	0.38	0.15	0.75	4.02
13	0.12	0.04	0.35	2.12

size and the area fraction of precipitates as Si content increased.

The size distributions of precipitates in the modified Zry-4 are shown in Fig. 3. Sizes of $Zr(Fe,Cr)_2$ and $Zr(Fe,Cr,Si)_2$ precipitates were mainly around 0.1 μm and always less than 0.3 μm. These precipitates were not as large as the largest Zr_2Si precipitates. The size of Zr_2Si precipitates ranged from 0.3 to 0.75 μm and the numbers of those were much smaller than that of $Zr(Fe,Cr)_2$ and $Zr(Fe,Cr,Si)_2$ precipitates. It should be noted that numerous precipitates less than 0.05 μm were observed in TEM study. However, these precipitates were excluded in calculations of the area fraction and the average size of precipitates due to the difficulty in observation. It is probable that these small precipitates less than 0.05 μm were important for oxidation and mechanical properties in zirconium alloys.

The critical stress needed to force passage of a dislocation line through precipitate array is given by $\sigma_s = 2Gb/\lambda$ [36,37], where G is the shear modulus, b the Burgers vector and λ the average spacing between the precipitates. The spacing can be obtained by $\lambda = (2rN)^{-1/2}$ where r is the radius of the precipitate and N the number of the precipitates per unit volume. The yield stress increase, calculated using $G = 35$ GPa [38], $b = 3.2 \times 10^{-8}$ cm [39] and the average radius of precipitate and the area fraction of precipitate shown in Table 3, ranged from 32 to 59 MPa as the silicon content increased from 0.01 to 0.1 wt% in the specimens with 1.5 wt% Sn. These values are smaller than those obtained from the tensile test by a factor of 10. Precipitates less than 0.05 μm in diameter were not included in calculating the stress (σ_s) and this indicates that precipitates smaller than 0.05 μm are important for mechanical properties of the modified Zry-4 alloys.

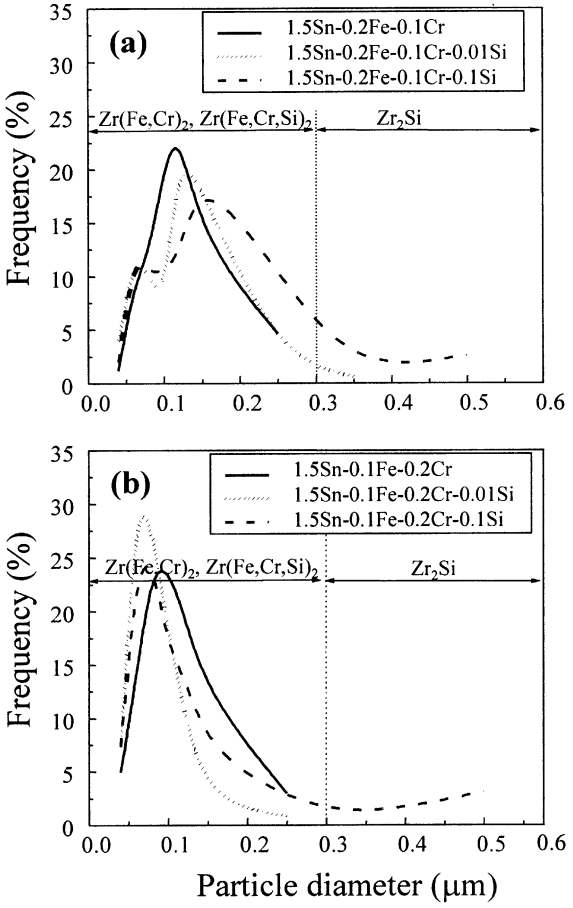

Fig. 3. Particle size distributions of precipitates in the modified Zry-4 alloys. (a) Zr–1.5Sn–0.2Fe–0.1Cr–xSi alloys, (b) Zr–1.5Sn–0.1Fe–0.2Cr–xSi alloys.

3.4. Oxide structure

In the authors' previous study, the oxide of Zry-4 in the pre-transition region was found to be a mixture of the tetragonal and monoclinic phases [9,12,14]. The amount of the tetragonal phase in the oxide, evaluated by the laser Raman spectroscopy, was around 40% before the rate transition. This tetragonal phase is believed to be more protective against oxidation than the monoclinic phase [18,19]. The inverse relationship of weight gain change with the fraction of tetragonal phase was observed in the previous study. When the weight gain increased, the tetragonal fraction decreased and this relationship was consistent throughout the specimens.

It is well known that alloying elements can influence the amount of the tetragonal phase. For example, Harada [40] investigated the effect of the tin content on the oxide structure. He reported that the oxide was composed of the monoclinic and tetragonal phase in the specimen less than 0.1 wt% tin; however, only the

monoclinic phase was observed in the specimen containing 2.2 wt% tin. Thus, he suggests that tin stabilizes the monoclinic phase. In the present study, the oxide structures of the Zr–Si binary specimens were investigated after 50 days exposure by Raman spectroscopy. The analysis showed that the oxide structure was a mixture of the tetragonal and monoclinic phase and the amount of the tetragonal phase was about 35% regardless of the silicon content. Thus, silicon additions in the present specimens do not seem to change the amount of the tetragonal phase of the oxide.

3.5. Grain structure

Fig. 4 shows the grain size change with the silicon content. The grain size of Zr–Si binary alloys decreased as the silicon content increased from 0 to 0.01 wt%. Further increases in silicon content to 0.05 and to 0.1 wt% resulted in a slight decrease of the grain size. It seems that grain growth was restricted by Zr_2Si precipitates at the grain boundaries. In the case of silicon-added modified Zry-4 alloys, the silicon addition did not significantly change the grain size. It is likely that the pinning effect of the precipitate is less effective than that of $Zr(Cr,Fe)_2$ precipitates and so the same grain size is obtained.

From the phase diagram of the Zr–Si system, silicon is found to extend the beta zirconium region and so acts as a beta zirconium stabilizer. In the present study, the optical microstructural observation of binary Zr–Si specimens showed no distinguishable changes in the final heat-treated microstructures (alpha annealed) with increasing silicon content from 0.01 to 0.1 wt%. Any trace of beta phase was not observed in all the specimens. The reason for this may be that the beta phase was entirely transformed to the alpha phase during the beta-quenching step or that any beta phase left over from the beta-quenching was transformed to the alpha phase during the following alpha annealing. Thus, silicon addition in the present study does not seem to affect the final alpha annealed microstructure and the subsequent oxidation resistance.

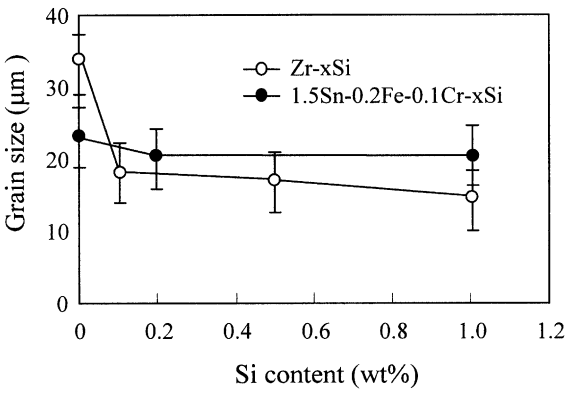

Fig. 4. Grain size variation with the silicon content in Zr–Si binary alloys and Zr–1.5Sn–0.1Fe–0.2Cr–Si alloys.

4. Conclusions

1. In autoclave tests for 100 days exposure at 360 °C, the measurement of weight gain in the modified Zry-4 alloys showed that small additions of silicon lowered the weight gain while further additions more than about 0.01 wt% increased the weight gain. So, the optimum silicon concentration for improved oxidation resistance is thought to be around 0.01 wt%.
2. The ultimate tensile strength of the modified Zry-4 increased with the increase in silicon content. However, 0.1 wt% silicon was not high enough to compensate the decrease in strength resulting from the reduction of the Sn content from 1.5 to 1.0 wt%.
3. For silicon-added modified Zry-4 specimens, two main precipitates were found to be $Zr(Fe,Cr)_2$/$Zr(Fe,Cr,Si)_2$ and Zr_2Si precipitates. For Zr–Si binary specimens, only one kind of Zr_2Si precipitate was observed. Sizes of $Zr(Fe,Cr)_2$ and $Zr(Fe,Cr,Si)_2$ precipitates were measured to be around 0.1 μm and were always less than Zr_2Si precipitates. In general, higher silicon contents show larger precipitates and higher area fraction. It is considered that the role of silicon in the precipitate of the present specimens is to form a binary zirconium-silicon precipitate or to replace Fe or Cr in the $Zr(Fe,Cr)_2$ precipitate, and thus to increase the size and the area fraction of precipitates.
4. In the TEM study, many small precipitates less than 0.05 μm were observed. The precipitates were uniformly distributed along the grain boundaries or within the grains. A comparison between the calculated and measured yield stress shows that it is probable that these small precipitates are important for oxidation and mechanical properties in the modified Zry-4 alloys.

Acknowledgements

This study was supported by Korea Electric Power Corporation (KEPCO) and Electrical Engineering and Science Research Institute (EESRI) and by the Brain Korea 21 Project.

References

[1] G.P. Sabol, G.R. Kilp, M.G. Balfour, E. Roberts, in: 8th Int. Symp. on Zirconium in the Nuclear Industry, vol. 1023, ASTM STP, 1989, p. 227.

[2] F. Garzarolli, H. Seidel, R. Tricot, J.P. Gros, in: 9th Int. Symp. on Zirconium in the Nuclear Industry, vol. 1132, ASTM STP, 1991, p. 395.
[3] H. Anada, K. Takeda, S. Hagi, International Topic Meeting on LWR Fuel Performance, Park City, USA, 10–13 April 2000, p. 445.
[4] D. Charquet, J.P. Gros, J.F. Wadier, International Topic Meeting on LWR Fuel Performance, Avignon, France, 21–24 April 1991, p. 143.
[5] F. Garzarolli, R. Schumann, E. Seinberg, in: 10th Int. Symp. on Zirconium in the Nuclear Industry, vol. 1245, ASTM STP, 1993, p. 709.
[6] G.P. Sabol, R.J. Comstock, U.P. Nayak, in: 12th Int. Symp. on Zirconium in the Nuclear Industry, vol. 1354, ASTM STP, 2000, p. 525.
[7] T. Isobe, Y. Matsuo, in: 9th Int. Symp. on Zirconium in the Nuclear Industry, vol. 1132, ASTM STP, 1991, p. 346.
[8] Y. Broy, F. Garzarolli, A. Seibold, L.F. Van Swam, in: 12th Int. Symp. on Zirconium in the Nuclear Industry, vol. 1354, ASTM STP, 2000, p. 609.
[9] H.S. Hong, S.J. Kim, K.S. Lee, J. Nucl. Mater. 238 (1996) 211.
[10] H.S. Hong, S.J. Kim, K.S. Lee, J. Nucl. Mater 257 (1998) 15.
[11] H.S. Hong, S.J. Kim, K.S. Lee, J. Nucl. Mater. 265 (1999) 108.
[12] H.S. Hong, S.J. Kim, K.S. Lee, J. Nucl. Mater. 273 (1999) 177.
[13] H.S. Hong, H.S. Kim, S.J. Kim, K.S. Lee, J. Nucl. Mater. 280 (2000) 230.
[14] H.S. Hong, S.J. Kim, K.S. Lee, J. Nucl. Mater. 297 (2001) 113.
[15] ASTM G-2, Standard Test Method for Corrosion Testing of Products of Zirconium, Hafnium, and Their Alloys in Water at 680 °F or in Steam at 750 °F, 1993, p. 47.
[16] D.R. Clark, F. Adar, J. Am. Ceram. Soc. 65 (1982) 284.
[17] R.C. Gavie, P.S. Nicholson, J. Am. Ceram. Soc. 55 (1972) 303.
[18] V.G. Keramidas, W.B. White, J. Am. Ceram. Soc. 57 (1974) 22.
[19] C.E. Ludin, Trans. Am. Soc. Metals 45 (1953) 901.
[20] H. Okamoto, Bull. Alloy Phase Diagrams 11 (1990) 513.
[21] T.B. Massalski, Binary Alloy Phase Diagrams, 2nd Ed., ASM, Metals Park, OH, 1990, p. 1511.
[22] R.P. Elliott, Constitution of Binary Alloys, McGraw-Hill, New York, 1965.
[23] J.B. Vanderssande, A.L. Bement, J. Nucl. Mater. 52 (1974) 115.
[24] V. Krasevec, J. Nucl. Mater. 98 (1981) 235.
[25] X. Meng, D. Northwood, J. Nucl. Mater. 132 (1985) 80.
[26] G. Lelievre, C. Tessier, X. Iltis, B. Berthier, F. Lefebvre, J. Alloys Comp. 268 (1998) 308.
[27] A. Drasner, Z. Blazina, J. Alloys Comp. 199 (1993) 101.
[28] O. Canet, M. Latroche, F. Boureevigneron, A. Percheronguegan, J. Alloys Comp 210 (1994) 129.
[29] D. Shaltiel, I. Jacob, D. Davidov, J. Less. Comm. Met. 53 (1976) 117.
[30] T.O. Malakhova, in: O.S. Ivanov (Ed.), Splavy At. Energ., Izd. Nauka Moskow, USSR, 1979, p. 123.
[31] D. Charquet, R. Hahn, E. Ortlieb, J. Gros, J. Wadier, in: 8th Int. Symp. on Zirconium in the Nuclear Industry, vol. 1023, ASTM STP, 1989, p. 405.
[32] I. Barin, O. Knacke, O. Kubaschewski, Thermodynamic Properties of Inorganic Substances, (Suppl. 1977), Springer, Berlin, 1973.
[33] O. Kubaschewski, C. Alcock, P.J. Spencer, Metallurgical Thermochemistry, 5th Ed., Pergamon, UK, 1979.
[34] O.J. Kleppa, S. Watanabe, Metall. Trans. B 13 (1982) 391.
[35] I. Ansara, A. Pasturel, K.H.J. Buschow, Phys. Status Solidi A 69 (1982) 447.
[36] D.R. Olander, Fundamental Aspects of Nuclear Reactor Fuel Elements, Sprinfield, Technical Information Center, 1976.
[37] J.W. Martin, Micromechanisms in Particle-Hardened Alloys, Cambridge University, Cambridge, 1980.
[38] B. Lustman, F. Kerze, The Metallurgy of Zirconium, McGraw-Hill, New York, 1955.
[39] J. Friedel, Dislocations, Pergamon, Oxford, 1964.
[40] M. Harada, M. Kimpara, K. Abe, in: 9th Int. Symp. on Zirconium in the Nuclear Industry, vol. 1132, ASTM STP, 1991, p. 368.